Cyclic fatigue demands on structures subjected to the 2010-2011Canterbury Earthquake Sequence

J.B. Mander

Texas A&M University, College Station, Texas, USA.

G.W. Rodgers

Dept. of Mechanical Engineering, University of Canterbury, Christchurch, NZ

2013 NZSEE Conference

ABSTRACT: The effect of low-cycle fatigue demands imposed by a sequence of earthquakes begs the question: For a given structure, what is the proportion of the available fatigue resistance consumed, and what is the remaining dependable fatigue-life, if any? The cumulative demand placed on structures subjected to the 2010-2011 Canterbury earthquake sequence is thus investigated and considers all major earthquakes (M5.0 or higher) that occurred. Results are presented as fatigue demand spectra for structures with natural periods from 0.1 to 5.0 seconds. For each structural period, time-history responses are normalised to an equivalent number of cycles at the seismic displacement amplitude specified for that period within two New Zealand Structural design loadings codes. The computed cyclic demand results are compared to the code-based expectation that seismic detailing should ensure a dependable cyclic loading capacity of 4 completely reversed cycles at the design spectral displacement amplitude. Results show that for many structures, the ideal 4-cycle capacity was exhausted prior to February 22, 2011 and for most structural types was exceeded by a significant margin following the February 22, 2011 Christchurch Earthquake.

1 INTRODUCTION

The Canterbury Earthquake Sequence has been unique in terms of the length and magnitude of the aftershocks. While there have been in excess of 10,000 recorded aftershocks, the significant aspect of the earthquake sequence on structures has been the more than 20 earthquake events with magnitude 5.0 or higher. Many of these events have been very close to the Central Business District (CBD) and induced local peak ground accelerations (PGAs) normally considered likely for larger magnitude events. The seismic demands of this unusual sequence of earthquakes have highlighted the need to better consider the cumulative cyclic damage effects that can be imposed on structures within the region.

The effects of low-cycle fatigue on civil engineered structures under earthquake loading are very important. Mechanical engineers are well versed in fatigue design considerations, often as the result of high-cycle fatigue from regularly fluctuating stresses on shafts in rotating machinery and vibrations on aircraft structures and other similar applications. However, due to the different application and the overall difficulty in defining the fatigue demand on a structure from wind and seismic loading, fatigue has not been so well incorporated into design practices within the civil engineering field. Although structural engineers are not explicitly required by code to design for low cycle fatigue effects, designers are required to be aware of the ramifications of low cycle fatigue. Some existing material covering seismic fatigue consideration is provided in Chang and Mander (1994), Dutta and Mander (2001), Dutta et al (1999) and Mander et al (1994).

This research takes the wealth of data available from the Canterbury Earthquake Sequence to investigate the cumulative cyclic demands on structures from the on-going seismic events. To limit the computational effort, this investigation considers all major earthquakes (M5.0 or higher) that occurred, from the September 4, 2010 main shock, up to an including the major shock of February 2011.

2 METHODS

2.1 Ground Motion Records

This research utilises the ground motion records for the major events from the September 4, 2010 M7.1 Darfield Earthquake, up to and including the February 22, 2011 M6.3 Christchurch Earthquake. These events are determined to be the magnitude 5.0 or higher. Due to large PGA readings within the CBD, the M4.9 the 2010 Boxing Day event has also been included. The recordings considered are for the four GeoNet Christchurch CBD recording stations. Specifically, these stations are the Christchurch Botanic Gardens (CBGS), Christchurch Cathedral College (CCCC), Christchurch Hospital (CHHC) and at Resthaven (REHS). For each event, Table 1 presents the GeoNet reference, the time of the event (in local time and UTC), the magnitude, the focal depth, and the distance from the epicentre to the recording station site.

Many of the results presented in Table 1 are obtained by processing and filtering the raw recording station outputs as most of these events were not available as processed records on the GeoNet ftp site at the time of processing. Absent fields indicate that no recording occurred at that station for that event. PGA values in Table 1 represent the peak horizontal acceleration from either orthogonal direction.

Table 1: Events considered in the cumulative demand analysis.

					CBGS		CCCC		CHHC		REHS	
GeoNet Ref.	Event Time (Local Time)	Event Time (UTC)	Mag	Depth (km)	PGA (%g)	Dist. (km)	PGA (%g)	Dist. (km)	PGA (%g)	Dist. (km)	PGA (%g)	Dist. (km)
3366146	Sat, Sep 4 2010 4:35 am	2010-09-03-1635	7.1	11	18.86	36	23.81	39	21.38	37	26.28	38
3366155	Sat, Sep 4 2010 4:56 am	2010-09-03-1656	5.3	8	0.29	32	-	34	-	32	1.01	33
3366230	Sat, Sep 4 2010 7:56 am	2010-09-03-1956	5.2	7	2.74	20	3.61	22	2.81	21	6.89	22
3366310	Sat, Sep 4 2010 11:12 am	2010-09-03-2312	5.3	12	0.81	28	1.21	31	-	29	-	30
3366313	Sat, Sep 4 2010 11:14 am	2010-09-03-2314	5.3	6	1.02	36	1.21	39	-	37	-	38
3366452	Sat, Sep 4 2010 4:55 pm	2010-09-04-0455	5.4	10	-	53	1.59	55	-	53	2.16	54
3367742	Mon, Sep 6 2010 11:24	2010-09-06-1124	5.2	9	1.71	19	2.82	21	2.11	20	5.65	20
3367749	Mon, Sep 6 2010 11:40	2010-09-06-1140	5.4	9	1.92	59	4.73	61	3.17	60	7.40	61
3367832	Tue, Sep 7 2010 3:24 am	2010-09-06-1524	5.4	15	1.85	33	3.73	35	2.81	34	6.28	35
3368445	Wed, Sep 8 2010 7:49 am	2010-09-07-1949	5.1	6	15.79	7.9	25.40	5.8	24.57	7.0	13.53	7.7
3382676	Mon, Oct 4 2010 10:21	2010-10-04-0921	5.0	12	1.64	13	2.91	15	1.84	14	4.27	15
3388384	Wed, Oct 13 2010 4:42	2010-10-13-0342	5.0	15	1.10	16	1.99	18	1.43	17	3.34	18
3391440	Tue, Oct 19 2010 11:32	2010-10-18-2232	5.0	9	7.30	12	17.51	12	10.43	12	9.04	13
	Sun, Dec 26 2010 10:30	2010-12-25-2130	4.9	5	35.54	2.1	22.36	1.7	25.49	1.4	24.40	2.7
3450113	Thu, Jan 20 2011 6:03 am	2011-01-19-1903	5.1	10	2.10	11	5.28	12	3.35	11	3.38	13
3468575	Tue, Feb 22 2011 12:51	2011-02-21-2351	6.3	5	53.06	11	49.31	8.5	36.73	9.8	71.82	10.4

2.2 Response Spectra Generation

Response spectra were generated for each of the recordings. Overall, there are two orthogonal horizontal directions for each recording station and each event. There are 16 major events listed in Table 1 and four recording stations considered per event. There are 8 total records omitted as there was no recording available for that event and recording station. This gives a total of 112 ground motion records available for the events listed in Table 1. For each recording, a response spectrum is generated with standard 5% inherent damping.

2.3 Calculation of Equivalent Cyclic Fatigue Demand

Due to the extensive amount of data available, it was necessary to find a reliable method to convert each displacement response into an equivalent number of fatigue cycles at a given reference amplitude. While there are some existing techniques to do this, specifically rain-flow analyses, these were deemed too computationally expensive and time consuming to set up. Instead two simple methods were investigated.

First, an area equivalence method was utilised, where the area between the displacement response vs time graph and the time-axis was integrated using a trapezoidal integration routine. This integrated area was then normalised by the area enclosed by one fully reversed sine-wave cycle at the period of interest and given normalisation amplitude. This method provides a simple to compute fatigue cycle equivalence.

Second, a normalisation routine, referred to herein as RMC, was applied at each calculated point using an approach akin to the well-known root-mean-square (RMS) signal analysis technique. This cycle equivalence approach is based upon inferring the peak displacement points throughout a time-history analysis at each change in direction of the structure and calculating an effective number of cycles for a given reference amplitude.

The specific cycle-counting approach is given by the effective amplitude, ε_i, at each displacement point which can be calculated relative to a given reference amplitude, A_{ref}:

$$\varepsilon_i = \left(\frac{|x_i|}{A_{ref}} \right)^C \tag{1}$$

where x_i is the i^{th} displacement points and C is the fatigue exponent.

The value of C is taken to be C = 1 for concrete-critical fatigue (Dutta and Mander, 2001), C = 2 for reinforcing-steel critical fatigue (Mander et al., 1994), and C = 3 which is also the well-known fatigue exponent for structural steel. Note that a value of C = 1.0 puts a weighting on each cycle that is directly proportional to its relative magnitude, whereas values of C = 2.0 and 3.0 put a much smaller weighting on small amplitude cycles and a much larger weighting on any response cycles that exceed the reference amplitude. Also note that for C = 2, RMC and RMS are equivalent.

The fatigue-weighted mean, m, of all displacement points can be determined from:

$$m = \frac{\sum_{i=1}^{N} \left(\frac{|x_i|}{A_{ref}} \right)^C}{n_{points}} \tag{2}$$

in which $n_{points} = t_f/\Delta t$ = the total number of points for that record, t_f = the final time for the record (the record length), and Δt = the time step for that record. This mean value can be transformed into an effective amplitude, based upon the integration of fully reversed sine-wave cycle. For C = 2, this analysis is the same as a root-mean-squared approach whereby the effective amplitude can be determined by multiplying the mean value by a multiplier B = $\sqrt{2}$. For C = 1, B = $\pi/2$ = 1.57 and for C = 3, B = 1.33. Therefore the effective amplitude becomes:

$$A_{eff} = Bm^{1/C} = B\left[\left(\frac{\sum_{i=1}^{N} \left(\frac{|x_i|}{A_{ref}} \right)^C}{n_{points}} \right)^{1/C} \right] \tag{3}$$

The effective number of fully reversed cycles at the current design period of interest can be determined from:

$$N_{cycles} = \frac{n_{points}\,\Delta t}{T} = \frac{t_f}{T} \tag{4}$$

where T is the natural period of the structure of interest. Finally, the number of effective cycles at the reference amplitude can be determined from:

$$N_{eff} = N_{cycles} \left(A_{eff} \right)^C \tag{5}$$

This final result presents the effective number of fully reversed response cycles (N_{eff}) at the effective amplitude A_{eff}. Both the area equivalence and RMC-type approach of Equation (5) were used to calculate the total equivalent number of fatigue cycles. Both methods gave similar results, thus verifying the data reduction methods used.

2.4 **Design Code Spectral Displacements**

When considering fatigue equivalence, it is important to have a reference cycle amplitude. The reference amplitude in this study is defined as the design code spectral displacement for the corresponding structural period. Two design codes are considered for comparison – NZS 4203:1984 and NZS1170.5:2004.

For NZS4203:1984, the spectral displacement from the code, based on Zone B – Soft soil for Chirstchurch, with ductility, μ = 4, from Figure 3 of NZS3101 and uniform force reduction factor, R = μ = 4 as per Newmark's well-known equal displacement factor. Taking peak maxima only and simplifying gives:

- For short-period structures, $T \leq 0.7$ s, $S_d = 0.12425\ T^2$
- For long-period structures, $T \geq 1.2$ s, $S_d = 0.07455\ T^2$
- For medium-period structures, $0.7 < T < 1.2$ s, $S_d = 0.1938\ T^2 - 0.0994\ T^3$

The elastic site hazard spectrum for NZS1170.5 is:

$$C(T) = C_h(T)\, Z\, R\, N(T, D) \qquad (6)$$

in which $C_h(T)$ = the spectral shape factor, Z = the hazard factor (= 0.22 for Christchurch), R = the return period factor (R = 1.0 for the 500-year return period design event) and N = the near-fault factor (N = 1.0 for Christchurch).

For Class D deep or soft soil, the spectral shape factor is given as:

Period Range	***Shape Factor***
$T < 0.1$	$C_h(T) = 1.12 + 1.88\,(T / 0.1)$
$0.1 \leq T < 0.56$	$C_h(T) = 3.0$
$0.56 \leq T \leq 1.5$	$C_h(T) = 2.4(0.75 / T)^{0.75}$
$1.5 < T \leq 3.0$	$C_h(T) = 2.14 / T$
$3.0 < T$	$C_h(T) = 6.42 / T^2$

(7)

Using Equations (6) and (7), it is possible to define the acceleration spectra. From this spectra, the displacement response spectra can be generated from:

$$S_d = \frac{g}{4\pi^2} S_a T^2 \qquad (8)$$

where S_d = the displacement response spectra (m); g = the acceleration due to gravity (g); S_a = the spectral acceleration (m/s^2); and T = the structural period (s).

Figure 1 presents a comparison between the displacement response spectra for Christchurch City, as defined by NZS4203 and NZS1170.5. It is evident that both codes have fairly similar requirements for spectral displacement at low periods, but that there is a notable deviation at higher periods, where NZS4203 allows much higher spectral displacement.

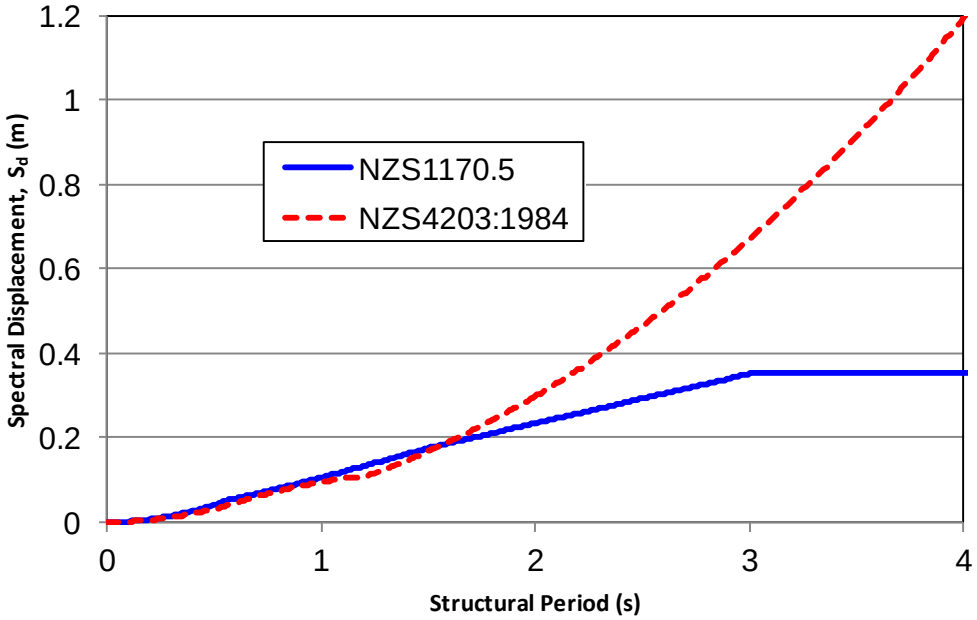

Figure 1: Displacement response spectra for NZS4203 and NZS1170.5.

2.5 **Response Spectra Normalisations**

Each response spectra is normalised in a number of ways to facilitate comparisons. Initially, each record is normalised to its own respective spectral displacement – dividing each displacement response record by the peak absolute value for that record. This normalisation is undertaken to provide a comparison between the effective duration of each earthquake irrespective of magnitude.

Each response spectra is then normalised to the design code spectral displacement (either from NZS4203:1984 or NZS1170.5) at the corresponding period. This analysis provides an estimate of the equivalent number of full design cycles that have occurred as a result of all considered ground motion records.

3 **RESULTS**

Figure 2 presents the effective number of cycles for each orthogonal ground motion record for every available recording station (from CBGS, CCCC, CHHC and REHS). In Figure 2 each result point was simulated and normalised to an effective amplitude, A_{eff}, equal to the spectral displacement for that specific record. Therefore, the results of Figure 2, present the record-to-record variability in terms of record duration and distribution of response cycle magnitude. The results of Figure 2 are plotted on a log-log scale. The log-normal mean (50^{th} percentile or median) and ± one log-normal standard deviation (16^{th} and 84^{th} percentiles) are presented on the graph as red lines. Presented in this way, the results provide an indication of the record-to-record variability, indicating the range of equivalent fatigue cycles, relative to the peak response for that record. Overall, Figure 2 presents 112 results for each period point, due to the two orthogonal horizontal directions for each available recording station and earthquake event, as shown in Table 1.

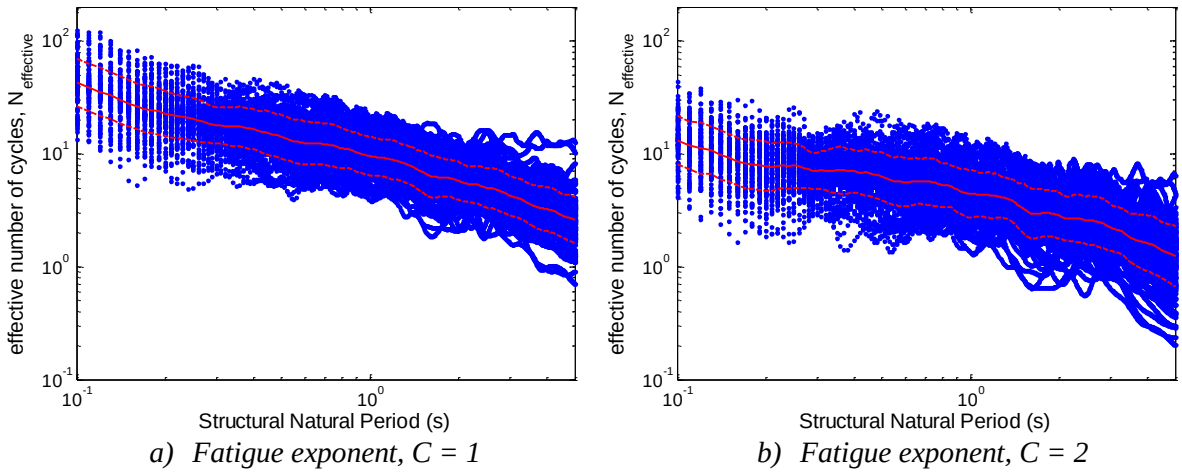

a) Fatigue exponent, C = 1

b) Fatigue exponent, C = 2

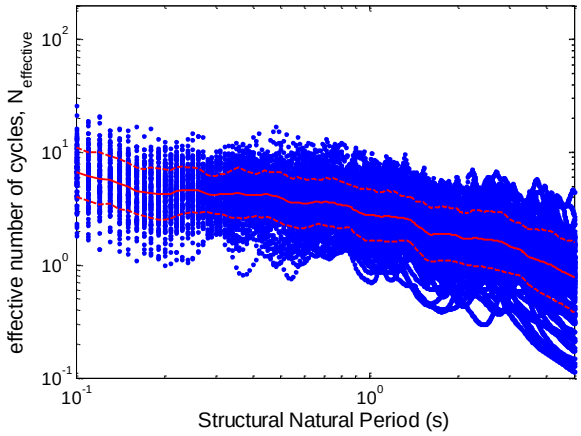

c) Fatigue exponent, C = 3

Figure 2: Number of effective cycles for each response with each record normalised to its own respective S_d. Each data point represents one orthogonal horizontal direction for one recording station and one earthquake event. The red lines overlaid represent the 16th, 50th and 84th percentile results.

Figure 3 presents the results where each record is normalised using a reference amplitude equal to the respective design code at the corresponding period. Results are presented for the design spectral displacement as defined in both NZS4203:1984 and NZS1170.5:2004 and using fatigue exponents, *C*, of 1, 2, and 3.

It can be seen that at low periods the equivalent number of cycles is very high, with the results up to and including the February 22, 2011 Christchurch Earthquake showing in excess of 100 cycles for the fatigue exponent of $C = 1.0$ in graphs a) and b) of Figure 3. This high number of cycles is due to the design code spectral displacement, which tends to zero at very low periods. The high number of cycles for $C = 1$ is reflective of the damage done on concrete materials.

For the fatigue exponent of $C = 2$, the peak number of cycles at low periods is notably lower with a maximum of approximately 30 equivalent cycles at low periods when normalised to NZS4203 in Figure 3c and approximately 20 equivalent cycles at low periods when normalised to NZS1170.5 in Figure 3d. At 1s natural period, the number of equivalent cycles is approximately 20-25 for both NZS4203 and NZS1170.5. This is reflective of the number of fatigue cycles imposed on reinforced concrete structures.

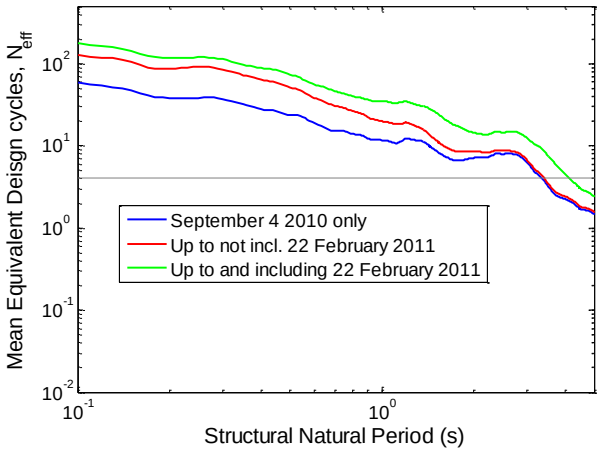

a) NZS4203 design code, fatigue exponent, C = 1

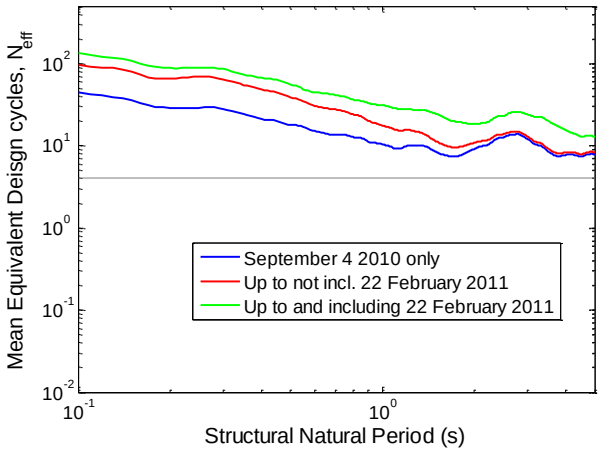

b) NZS1170.5 design code cycles, fatigue exponent, C = 1

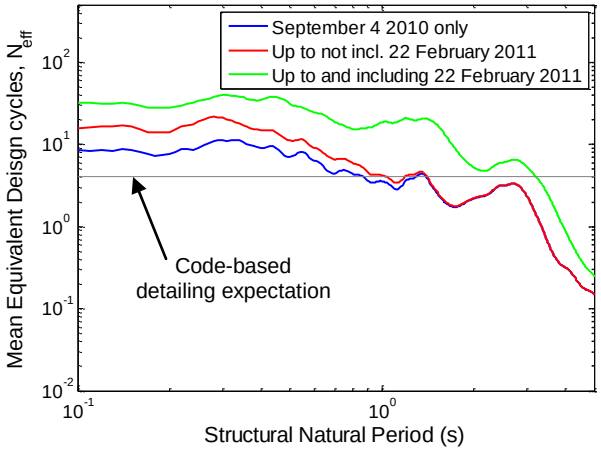

c) NZS4203 design code, fatigue exponent, C = 2

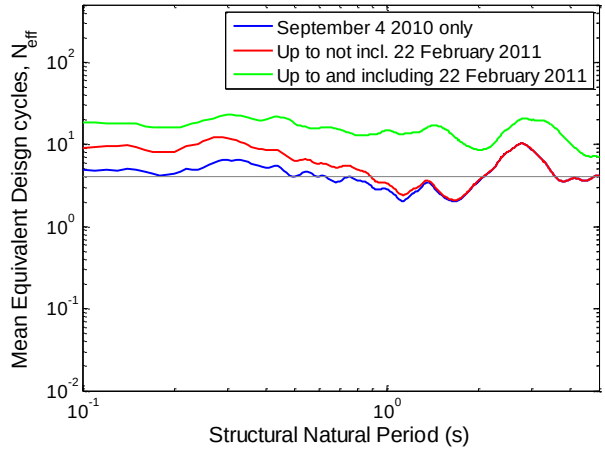

d) NZS1170.5 design code cycles, fatigue exponent, C = 2

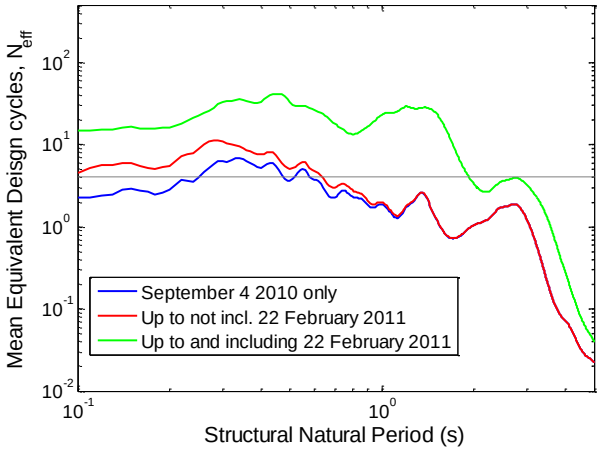

e) NZS4203 design code, fatigue exponent, C = 3

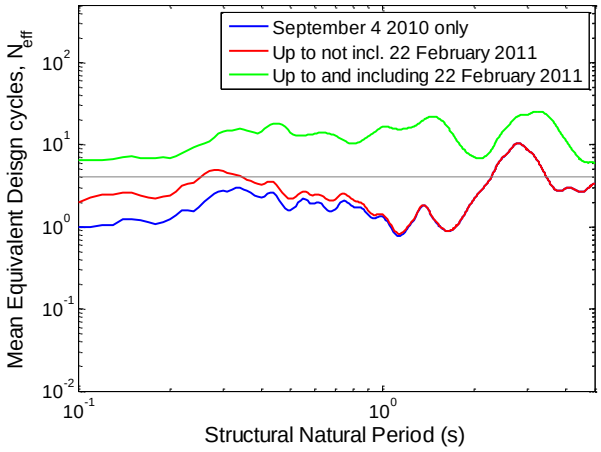

f) NZS1170.5 design code cycles, fatigue exponent, C = 3

Figure 3: Total number of equivalent design code cycles for different fatigue exponents.

For the fatigue exponent of $C = 3$, the number of equivalent cycles is much lower at short periods. It is important to note that the higher fatigue exponent puts a much higher importance on the large response cycles, and smaller cycles are almost excluded as they tend towards zero. For C = 3, the results are reflective of the number of damaging fatigue cycles imposed on structural steel systems. It is also evident in Figure 3 that the higher the fatigue exponent, the less additional cycles are included from all of the smaller events between the September 2010 and February 2011 main shocks, particularly at longer periods.

4 DISCUSSION

Each graph in Figure 3 also shows a horizontal line at 4 cycles. Below this threshold is considered to be the number of cycles in which dependable seismic performance can be assured as per the commentary in the loadings code NZS4203. Most structural element types along with associated connection details have been proof tested to indicate that dependable seismic performance can be assured to provide four completely reversed cycles at a ductility factor of 4 without more than 20% reduction in lateral load resistance.

Thus, according to Figure 3, most structures with a fundamental period of less than about 1 second had their dependable fatigue resistance consumed and exceeded by the Boxing Day earthquake of December 26, 2010. Following the main event on February 22, 2011 the cyclic fatigue demand exceeded the cyclic capacity by a wide margin for both reinforced concrete ($C = 2$, Figure 3d) and steel structures ($C = 3$, Figure 3f). It should be noted that such exceedance does not necessarily indicate or imply collapse, but rather that the ongoing structural reliability is undependable. In particular, this observation has serious ramifications relating to the post-disaster serviceability and safety of all structures in the affected region. Moreover, fatigue damage, by its very nature is generally irreparable damage, at least in the locally affected zones of members, particularly joints. Consequently, restoring the pre-damage (pre-earthquake) structural integrity and reliability that is demanded by insurance policy owners is a challenging, if not near impossible, task for most structures.

5 CONCLUSION

The cumulative fatigue demands imposed on structures as a result of the 2010-2011 Canterbury Earthquake Sequence has generally exceeded the dependable (4-cycle) fatigue capacity by a significant margin. In fact for reinforced concrete structures, the expected performance limits would have been met prior to the devastating February 22, 2011 Christchurch Earthquake. It is therefore not surprising that a significant proportion of structures have had to have been razed due to irreparable and often unseen fatigue damage as a consequence of the 2011 Christchurch Earthquake.

6 REFERENCES

Chang, G.A. and Mander, J. B. (1994). "Seismic energy based fatigue damage analysis of bridge columns: Part 2: Evaluation of seismic demand." Technical Report, NCEER-94-0013, *National Center for Earthquake Engineering Research, Buffalo, N.Y.*

Dutta, A. and Mander, J. B. (2001). "Energy based methodology for ductile design of concrete columns." *Journal of Structural Engineering* **127**(12): 1374-1381.

Dutta, A., Mander, J. B. and Kokorina, T. (1999). "Retrofit for control and repairability of damage." *Earthquake Spectra* **15**(4): 657-679.

Mander, J., Panthaki, F. and Kasalanati, A. (1994). "Low-Cycle Fatigue Behavior of Reinforcing Steel." *Journal of Materials in Civil Engineering* **6**(4): 453-468.

NZS 1170.5:2004 “Structural Design Actions, Part 5, Earthquake actions - New Zealand”, Standards New Zealand.

NZS 4203:1984 “Code of practice for General Structural Design and Design Loadings for Buildings”, Standards New Zealand.